

AD-A066 780

TUFTS UNIV MEDFORD MASS DEPT OF PHYSICS

F/G 3/2

VERY LARGE ARRAY (V.L.A.) OBSERVATIONS OF SOLAR ACTIVE REGIONS.(U)

FEB 79 K R LANG

F19628-79-C-0010

UNCLASSIFIED

SCIENTIFIC-1

AFGL-TR-79-0037

NL

OF
AD
A066780



AFGL-TR-79-0037

LEVEL

12
F

AD A0 66780

DDC FILE COPY

VERY LARGE ARRAY (V.L.A.) OBSERVATIONS OF SOLAR ACTIVE REGIONS

Kenneth R. Lang

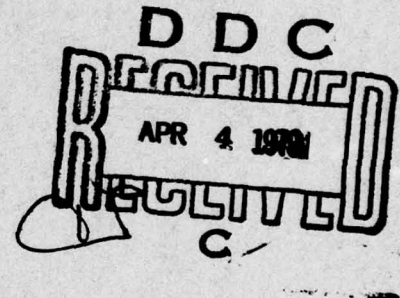
Department of Physics
Tufts University
Medford, Massachusetts 02155

Scientific Report No. 1

1 February 1979

Approved for public release; distribution unlimited

AIR FORCE GEOPHYSICS LABORATORY
AIR FORCE SYSTEMS COMMAND
UNITED STATES AIR FORCE
HANSCOM AFB, MASSACHUSETTS 01731



79 04 03 059

Qualified requestors may obtain additional copies from the Defense Documentation Center. All others should apply to the National Technical Information Service.

19 REPORT DOCUMENTATION PAGE		READ INSTRUCTIONS BEFORE COMPLETING FORM	
1. REPORT NUMBER AFGL-TR-79-00371	2. GOVT ACCESSION NO.	3. PRICE (if applicable)	4. CATALOG NUMBER
5. TITLE (and Subtitle) Very Large Array (V.L.A.) Observations of Solar Active Regions.		6. TYPE OF REPORT & PERIOD COVERED Scientific Report No. 1 15 Oct. 1978 - 1 Feb. 1979	
7. AUTHOR(s) Kenneth R. Lang		8. CONTRACT OR GRANT NUMBER(s) F 19628-79-C-0010	
9. PERFORMING ORGANIZATION NAME AND ADDRESS Department of Physics, Tufts University Medford, MA 02155		10. PROGRAM ELEMENT, PROJECT, TASK AREA & WORK UNIT NUMBERS 61102F 231100-30	
11. CONTROLLING OFFICE NAME AND ADDRESS Air Force Geophysics Laboratory Hanscom AFB, Massachusetts 01731 Contract Monitor: Donald Guidice/PHP		12. REPORT DATE 1 Feb 1979	
14. MONITORING AGENCY NAME & ADDRESS (if different from Controlling Office) 12-19p.		13. NUMBER OF PAGES 18	
15. SECURITY CLASS. (of this report) Unclassified		16. DECLASSIFICATION/DOWNGRADING SCHEDULE	
17. DISTRIBUTION STATEMENT (of this Report) Approved for public release, distribution unlimited. 14 SCIENTIFIC-1			
18. DISTRIBUTION STATEMENT (of the abstract entered in Block 20, if different from Report)			
19. SUPPLEMENTARY NOTES This paper has been accepted for publication in the journal <u>Nature</u>			
20. KEY WORDS (Continue on reverse side if necessary and identify by block number) Solar Radio Interferometry, Very Large Array, u-v Coverage, Fine Angular Scales, Flare Prediction, Active Sun, Coronal Magnetic Fields, Magnetograms, Circularly Polarized Radio Emission.			
21. ABSTRACT (Continue on reverse side if necessary and identify by block number) High resolution radio wavelength observations of solar active regions indicate ever present, fine scale features whose high degree of circular polarization reflects the magnetic field structure in the solar corona. Changes in this structure may trigger major flare eruptions in solar active regions which create geophysical disturbances and disrupt terrestrial communication and surveillance systems. In this paper we discuss the basic			

20. (cont.)

techniques of using the Very Large Array (V.L.A.) to obtain radio wavelength observations (6 cm) maps of solar active regions. It is shown that the V.L.A. coverage in the u-v plane (the Fourier plane of the active region's brightness distribution) is much more complete than the u-v coverage available with other synthesis telescopes or with interferometers with east-west baseline configurations. Calibration procedures for V.L.A. observations of the Sun are discussed, and maps of two solar active regions are presented. For the first time radio wavelength maps of coronal magnetic field structures have been obtained with angular resolutions comparable to those obtained at optical wavelengths when viewing the cooler, lower lying photosphere. The V.L.A. maps show small scale (< 30 seconds of arc) circularly polarized ($\sim 70\%$) sources which are thought to trigger solar flare emission. The 10^6 °K brightness temperature of these sources indicates that they belong to the coronal regions of the solar atmosphere, and the circular polarization indicates magnetic field strengths of a few hundred gauss. The general shape, orientation, and dipolar structure of the coronal magnetic fields (inferred from the V.L.A. maps) is shown to agree with similar features in the lower lying photosphere (inferred from optical wavelength magnetograms - Zeeman effect).

ACCESSION for	
NTIS	White Section <input checked="" type="checkbox"/>
DOC	Buff Section <input type="checkbox"/>
UNANNOUNCED	
JUSTIFICATION	
BY	
DISTRIBUTION/AVAILABILITY CODES	
<div style="display: flex; justify-content: space-between;"> 10 11 </div>	
<div style="display: flex; justify-content: space-between;"> A </div>	

Observations of the Sun with three element interferometers at centimeter wavelengths and angular resolutions of a few seconds of arc have shown that solar active regions contain intense (10^5 - 10^6 K), small-scale (less than 15"), circularly polarized (above 30%) sources which dominate solar emission at these wavelengths and angular resolutions.^{1,2} The radiation from these sources has been interpreted in terms of gyro-magnetic processes involving strong magnetic fields and thermal electrons in the dense coronal regions above sunspots.²⁻⁶ As long as the active regions are not emitting flares, the intensity, angular size, and degree of circular polarization of the small-scale sources remain remarkably constant for intervals of at least 12h. This stability makes these solar sources ideal candidates for the aperture synthesis technique which has been developed by radio astronomers to obtain two-dimensional maps of celestial radio sources with second of arc angular resolution.⁷ When applied to the centimeter wavelength radiation of the Sun, these techniques may be used to test the gyro-resonance absorption theory of this component of solar emission. Moreover, the synthesis technique can be used to obtain high resolution maps of circular polarization which delineate the magnetic field structure in the solar corona. These structures can then be compared with optical wavelength Zeeman effect observations of the magnetic field in the underlying photosphere and chromosphere. Because of scintillations in the terrestrial atmosphere, these optical wavelength observations are limited to the angular resolutions which are now available at radio wavelengths using the synthesis technique. The first synthesis maps of solar active regions at centimeter wavelengths were obtained using the twelve 25m paraboloids (20 interferometer pairs) of the Westerbork synthesis radio telescope.^{8,9} In this case, a synthesized beam of 6" X 22" at a wavelength

of 6 cm was used to show that solar active regions contain small-scale sources (with peak brightness temperatures as large as 10^6 K and circular polarizations of about 50%) surrounded by a lower intensity $\sim 10^5$ K halo. Although circularly polarized emission was observed from both sunspots and plage peaks, the more intense emission came from sunspots whose magnetic polarity coincided with the direction of circular polarization. In this paper we describe synthesis maps of solar active regions obtained using twelve 25m paraboloids (65 interferometer pairs) of the Very Large Array (V.L.A.) now under construction near Socorro, New Mexico by the National Radio Astronomy Observatory.¹⁰ In this case a synthesized beam of $1'' \times 3''$ is obtained at a wavelength of 6 cm. Here we describe the present and future observational capabilities of the V.L.A., and, we also describe the basic techniques of using the V.L.A. to observe the Sun. In addition, we present the first V.L.A. synthesis maps of solar active regions.

A total of 27 antennas are presently being constructed, tested and placed along the three arms of the WYE configuration of the V.L.A. The position angles of the north, southeast, and southwest arms are, respectively, 355° , 115° and 236° ; whereas the geodetic coordinates of the array center are $34^\circ 04' 43.497''$ north (latitude) and $107^\circ 37' 03.819''$ west (longitude). With this configuration and location the most complete spatial frequency coverage is obtained when the Sun is at its larger positive declinations. The permanent antenna stations are placed along each arm at distances ranging between 0.045 and 21.000 km from the array center, thereby providing effective angular resolutions ranging between $0.57''$ and $4.44''$ at a signal wavelength of 6 cm for the interferometer pairs along each arm (each combination of two antennae makes one interferometer pair). Similar angular resolutions are available for the interferometer pairs consisting of antennae

placed on different arms. The individual antennae have 25 m diameter main reflectors with a feed system¹¹ designed to receive signal wavelengths of 1.3 cm, 2 cm, 6 cm or 21 cm with respective beamwidths of 1.9', 2.9', 8.6' and 30' and respective aperture efficiencies of 46%, 54%, 65% and 50%. About one minute is required to rotate the antenna feeds to sample signals at different wavelengths. Two independent systems simultaneously accept two oppositely polarized signals at the chosen wavelength, and these signals are converted into intermediate frequency (I.F.) signals with bandwidths of 1.5 MHz, 12 MHz or 50 MHz. The two I.F. signals received at each antenna are sent to a central location where they are multiplied together to give the correlated flux for each oppositely polarized signal for every interferometer pair. Each correlated signal is time averaged to give its amplitude and phase every ten seconds of time.

The present digital system of the V.L.A. is designed to handle up to 12 antennas with two I.F. signals each, but more sophisticated electronics designed to handle 27 antennas with four I.F. channels each is now being installed. For the observations reported here we used twelve antennae with three antennae positioned along the southeast arm at 0.080, 0.090 and 0.147 km from the array center and nine antennae placed along the southwest arm at 0.045, 0.484, 0.710, 0.970, 1.589, 3.188, 5.223, 7.659 and 10.473 km from the array center. Altogether the average correlated flux from a total of 55 interferometer pairs was sampled every 30 sec at a signal wavelength of 6 cm for both the left hand circularly polarized (LCP) and right hand circularly polarized (RCP) signals. When observing the Sun at centimeter wavelengths the system noise is completely dominated by the solar brightness temperature of 10^4 - 10^6 K. The theoretical

r.m.s. noise fluctuation in the correlated flux density obtained with each antenna pair is 6.4 Jy ($1 \text{ Jy} = 10^{-23} \text{ erg s}^{-1} \text{ cm}^{-2} \text{ Hz}^{-1} = 10^{-26} \text{ W m}^{-2} \text{ Hz}^{-1}$) for a system noise temperature of 10^4 K with our chosen bandwidth of 12 MHz and an integration time of 30 s. We later averaged the data over 5 minute intervals to obtain a r.m.s. noise of 2 Jy for each interferometer pair.

Active regions 1046 (S 24° W 7° at 12^{h} U.T. on March 30) and 1056 (N 12° E 65° at 0^{h} U.T. on March 31) were respectively observed on March 30 and April 1, 1978 at a signal wavelength of 6 cm. For each antenna pair the correlator outputs were calibrated by observing 3C 84 or CTA 102 for five minutes every twenty minutes, whereas the solar active region was observed during the other fifteen minutes of each twenty-minute period. The frequent observations of the calibrator sources served to lessen the effects of tropospheric refraction variations, and to calibrate the instrumental gain, polarization and phase fluctuations.

For each polarization of each antenna pair the correlated flux, $S_{mn}(\text{sun})$, and the corrected phase $(\phi_m^* - \phi_n^*) - (\phi_m - \phi_n)$ when observing the Sun were taken to be the amplitude and phase of the visibility function, $V(u,v)$. Because corrections for the motion of the Sun across the sky, its rotation about its axis, and its horizontal parallax were incorporated in the computer program which determined the pointing of each antenna, the changing values of the visibility function could then be used to measure the brightness distribution of the active region $I(x,y)$, through the fundamental Fourier transform relation

$$V(u,v) = I(x,y) \exp[+2\pi i (ux + vy)] \, dx dy, \quad (1)$$

where the visibility function and the brightness distribution are

determined separately for the two circular polarizations, u and v are the projections of the baseline vector in the direction of increasing right ascension and declination, respectively; and x and y are, respectively, coordinates in the direction parallel to increasing right ascension and declination. These quantities, defined in radians, are given by

$$\begin{aligned} u &= B_x \sin(h) - B_y \cos(h) \\ v &= -B_x \sin(\delta) \cos(h) - B_y \sin(\delta) \sin(h) + B_z \cos(\delta), \end{aligned} \quad (2)$$

where B_x , B_y and B_z are the topocentric coordinates of the baseline vector in units of the observation wavelength, and h and δ respectively denote the hour angle and declination of the active region.

As the earth rotates, the hour angle of the active region changes and the projected baseline describes an ellipse in the u - v plane (the Fourier plane of the brightness distribution). The extent of the coverage in the u - v plane depends upon the Sun's declination, the orientation and length of the baseline vector of each interferometer pair, and the total number of interferometer pairs. During the observations reported here, for example, the Sun was near the vernal equinox when the Sun's declination passes through zero degrees, and the elliptical u - v tracks degenerate into straight lines. Figure 1 illustrates the u - v tracks when the Sun is observed at zero degrees declination with the Very Large Array (V.L.A.) and with interferometers which are oriented in a strictly east-west direction such as the Westerbork Synthesis Radio Telescope (W.S.R.T.). For the east-west baselines the v becomes zero for a declination of zero degrees. Later in the summer or winter, when the Sun's declination can respectively reach $+23^\circ$ and -23° , the extent of the v coverage by the W.S.R.T. broadens. For the V.L.A., the straight lines given in Figure 1

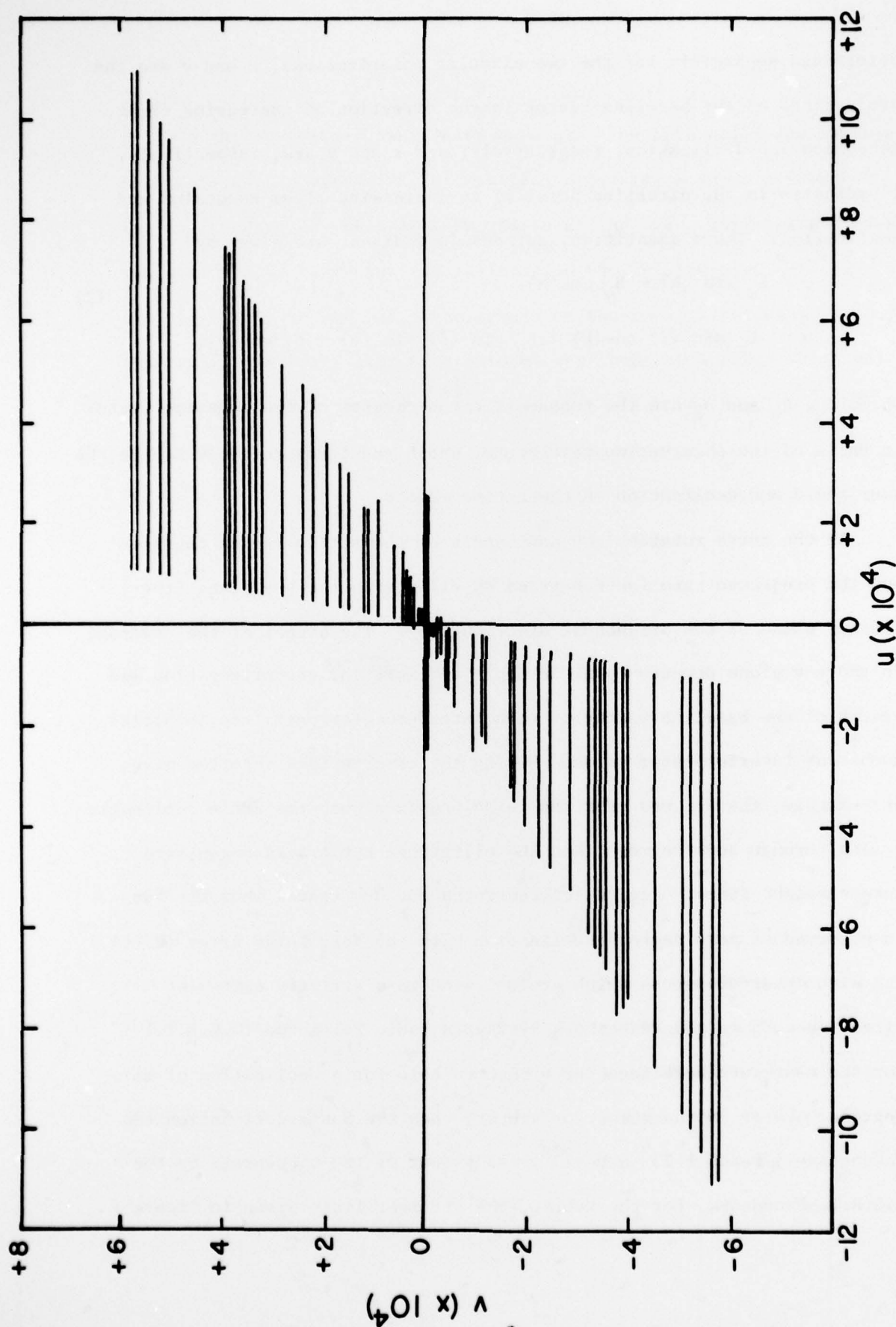


Figure 1. The $u-v$ tracks obtained while observing the Sun at 6 cm wavelength with 45 interferometer pairs of the V.L.A. when the Sun is at a declination of zero degrees. Because the longer baselines were not used in our maps, we have omitted here the ten tracks from the ten interferometer pairs connecting to the furthestmost antenna located at 10.473 km from the array center. The dark line at $v=0$ denotes the tracks obtained while observing the Sun at 6 cm wavelength with the 20 interferometer pairs of the W.R.S.T. when the Sun is at a declination of zero degrees.

become shortened or lengthened ellipses, respectively, for the southern and northern declinations.

The correlated flux when observing the Sun for each polarization with each antenna pair (m,n) was determined from the equation

$$S_{mn}(\text{sun}) = \frac{R_{mn}(\text{sun})}{R_{mn}(\text{cal})} \frac{[T_{sm}(\text{sun})T_{sn}(\text{sun})]^{\frac{1}{2}}}{[T_{sm}(\text{cal})T_{sn}(\text{cal})]^{\frac{1}{2}}} S_{mn}(\text{cal}) \exp[i(\phi_m^* - \phi_n) - i(\phi_n^* - \phi_m)], \quad (3)$$

where R_{mn} denotes the correlation coefficient (fraction of the total power which is correlated) for one polarization of the antenna pair (m,n).

$$R_{mn}(\text{cal}) = G_m G_n \frac{S_{mn}(\text{cal})}{[T_{sm}(\text{cal}) T_{sn}(\text{cal})]^{\frac{1}{2}}} \exp [i(\phi_m - \phi_n)], \quad (4)$$

where G_m and ϕ_m respectively denote the magnitude and phase of the complex gain of the detection system of antenna, m, the $S_{mn}(\text{cal})$ is the correlated flux when observing the calibration source with one polarization of the antenna pair (m,n), and $T_{sm}(\text{cal})$ denotes the system noise temperature when observing the calibrator source with one polarization of antenna, m.

When observing the solar active region the correlation coefficient, $R_{mn}(\text{sun})$, for one polarization of the antenna pair (m,n) is given by

$$R_{mn}(\text{sun}) = G_m^* G_n^* \frac{S_{mn}(\text{sun})}{[T_{sm}(\text{sun}) T_{sn}(\text{sun})]^{\frac{1}{2}}} \exp [i(\phi_m^* - \phi_n^*)]. \quad (5)$$

Because the parametric amplifiers were used for both solar and calibration observations, an extra I.F. attenuation producing a phase difference $(\phi_m^* - \phi_m)$ had to be inserted when observing the Sun. This phase difference was measured by observing the calibration source with each antenna with the attenuator in and out. The levels of the two I.F. signals being fed into each multiplier from each antenna were kept at a fixed value using an automatic level control (a.l.c.) loop in which the sampled signal level controls an attenuator in the final I.F. amplifier. The a.l.c. loop therefore automatically compensates for the variation in gain magnitude caused by the introduction of an extra I.F. attenuator when observing the Sun. This meant that we could assume that the gain magnitudes are the same when observing the calibrator and the sun ($G_m = G_m^*$). The system noise temperature, $T_{sm}(\text{cal})$, when observing the calibrator was measured for each antenna using a switched noise source whose temperature of $\sim 3\text{K}$ was accurately calibrated for each antenna by observing the Moon. The system noise temperature, $T_{sm}(\text{sun})$, when observing the active region was measured for each antenna by determining the difference in the total power detected when observing the active region and a quiet sun region whose temperature was assumed to be 10^4 K . Even at these high temperatures the front-end amplifiers were in their linear, unsaturated regions. Subsequent observations of more intense active regions with antenna temperatures $\sim 10^5\text{ K}$ did, however, require the removal of the parametric amplifiers in order to avoid saturation. In this case the gain and phase could be calibrated by observing 3C 273 with the amplifiers out, but it also had to be observed with the amplifiers replaced in order to measure the system noise temperatures, $T_{sm}(\text{cal})$.

The correlated flux of the calibration source, $S_{mn}(\text{cal})$, was taken to be 49 Jy and 34 Jy, respectively, when observing 3C 84 and CTA 102. The gain of each circularly polarized channel was calibrated by adjusting the digitized output of the correlators to give the same values of $R_{mn}(\text{cal})$ for every baseline pair and both polarizations. This is essentially because the calibrator sources have negligible circular polarization and they are effectively point sources for the interferometric baselines used. These instrumental adjustments were also applied to the solar data to obtain the corrected amplitude, $S_{mn}(\text{sun})$, and the corrected phase $(\phi_m^* - \phi_n^*) - (\phi_m - \phi_n)$ for each polarization of each antenna pair every 30 seconds of each 15 minute period of solar observations. The 30 second values of amplitude and phase were then added together to obtain five minute vector averages with a phase calibration better than 5° and an amplitude calibration accurate to less than 10%. These calibrated data were taken to be the amplitude and phase of the source visibility function, and the source intensity distribution was obtained by Fourier transforming the calibrated data using the Tufts University DEC-10 computer.

The procedure we have implemented involves a direct synthesis of a "dirty" map which is the convolution of the true brightness distribution with the response function of a point source. This response function, or "dirty beam" is illustrated in Figure 2. It has a full width to half maximum of $1'' \times 3''$, and the highest sidelobe is 14% of the maximum response.

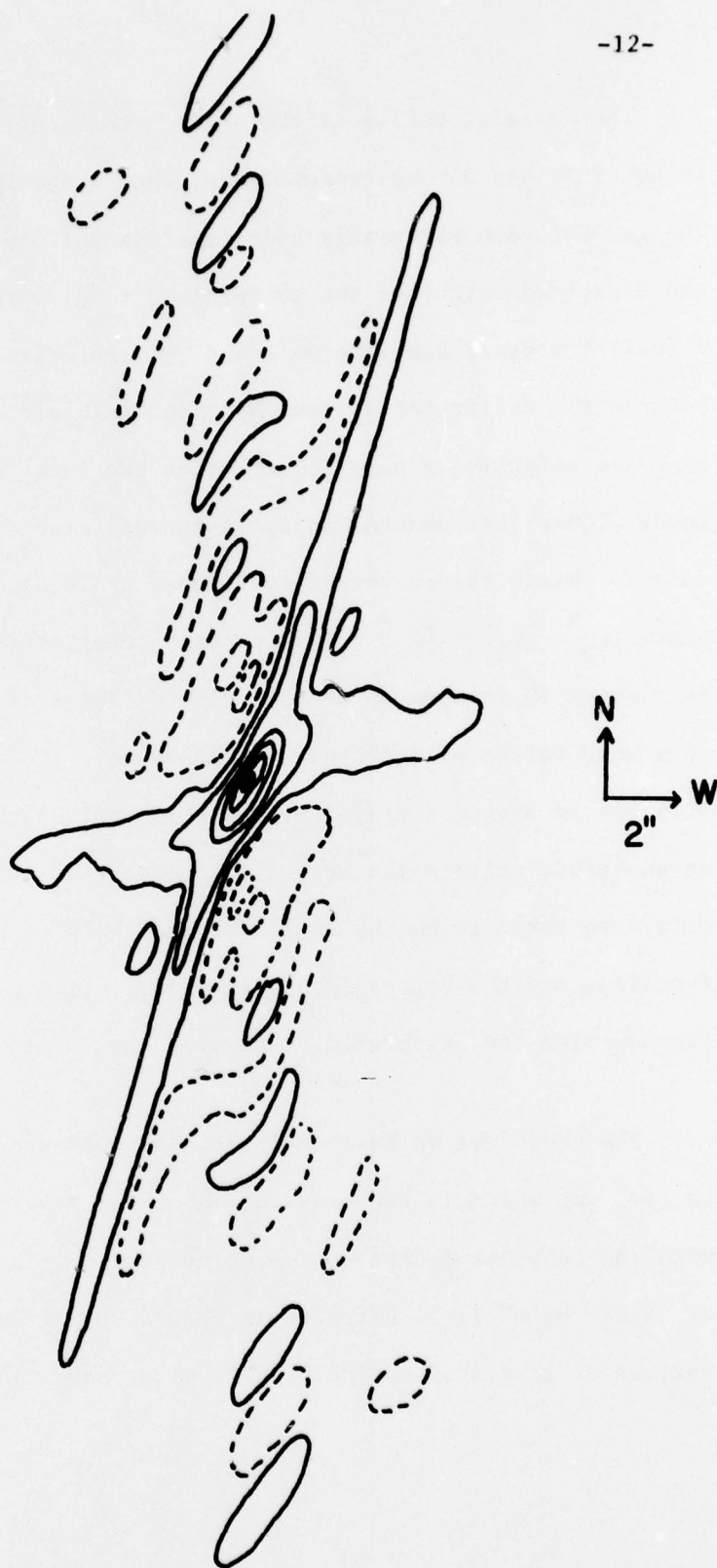


Figure 2. The "dirty" V.L.A. beam pattern at a signal wavelength of 6 cm constructed from observations during the daylight hours on April 1, 1978.

A deconvolution of the "dirty" map was then performed by means of the "clean" procedure in which the effects of the 14% sidelobes of the synthesized beam were reduced.¹² Because both active regions observed were resolved on baselines having fringe spacings less than 15" we have deleted those data having fringe spacings less than this value; thereby minimizing the map noise and reducing computer time. The resultant total intensity contour maps are shown in Figures 3 and 4, where the synthesized beam is represented by a shaded ellipse. Here the contour levels represent 0.9, 0.8, 0.7, 0.6, 0.5, ... 0.2 times the maximum response which had the values of 102, 80, 17 and 5 Jy per synthesized beam area (in units of square seconds of arc), respectively, for AR 1046 (LCP), AR 1046 (RCP), AR 1056 (RCP) and AR 1056 (LCP). The r.m.s. sensitivity of the V.L.A. system for 12 hours of observation of a 10^4 K Sun is estimated to be 0.6 Jy.

The most striking aspect of the maps shown in Figures 3 and 4 is that the small-scale sources shown in the LCP and RCP maps are not spatially coincident. They suggest the feet of small dipole magnetic fields with positive magnetic polarity corresponding to the regions with strong right circular polarization. Region 1046, for example, contains two sources $\sim 30'' \times 30''$ in size which are $\sim 80\%$ left circularly polarized with one source of similar angular size and $\sim 60\%$ right circular polarization located between them. Region 1056 contains one intense component about $30'' \times 30''$ in angular size with $\sim 70\%$ circular polarization. In all cases the small-scale sources are surrounded by less intense halo emission $\sim 1'$ in angular extent (large angular sizes $> 1'$ are undersampled by the V.L.A. system). Assuming a source size

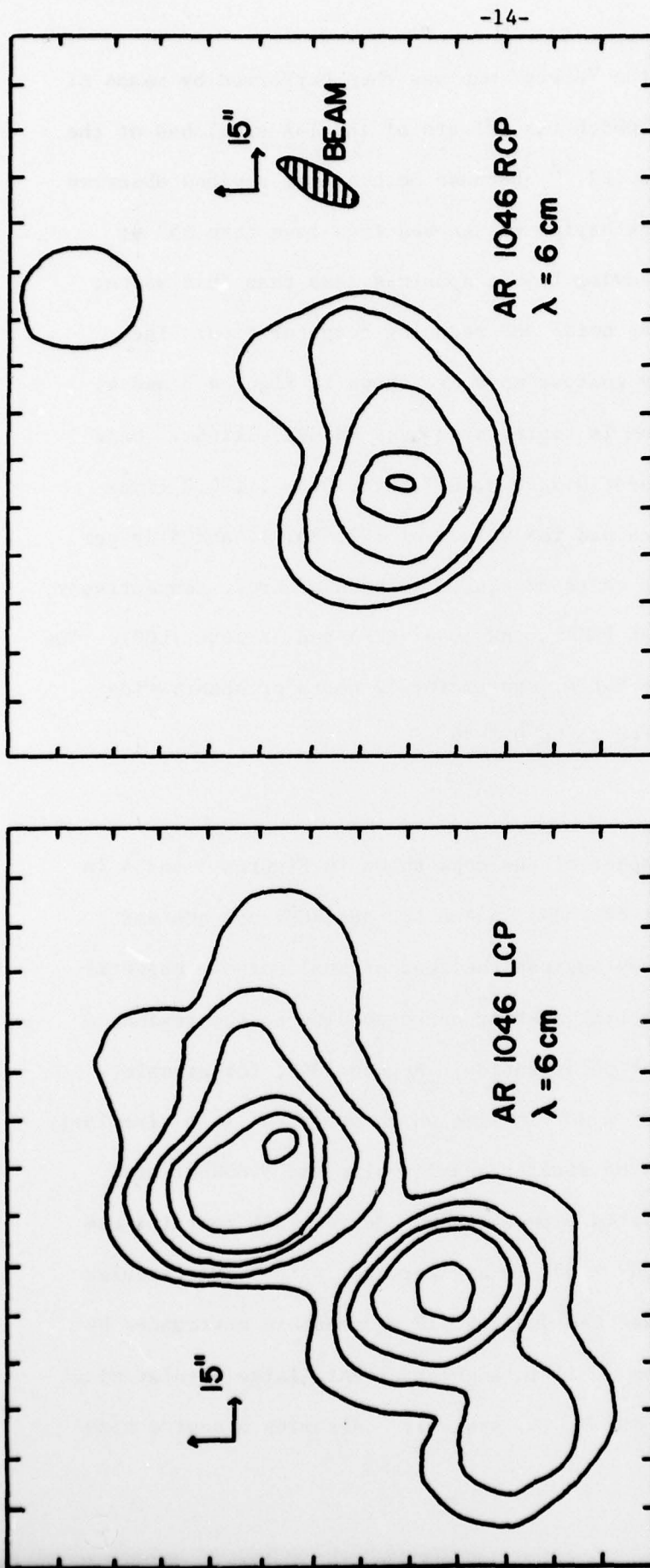


Figure 3. V.L.A. synthesis maps of solar active region 1046 obtained with one day's observation on March 30, 1978. Here, north is up, west is to the right, and LCP and RCP respectively denote the left and right hand circularly polarized signals.

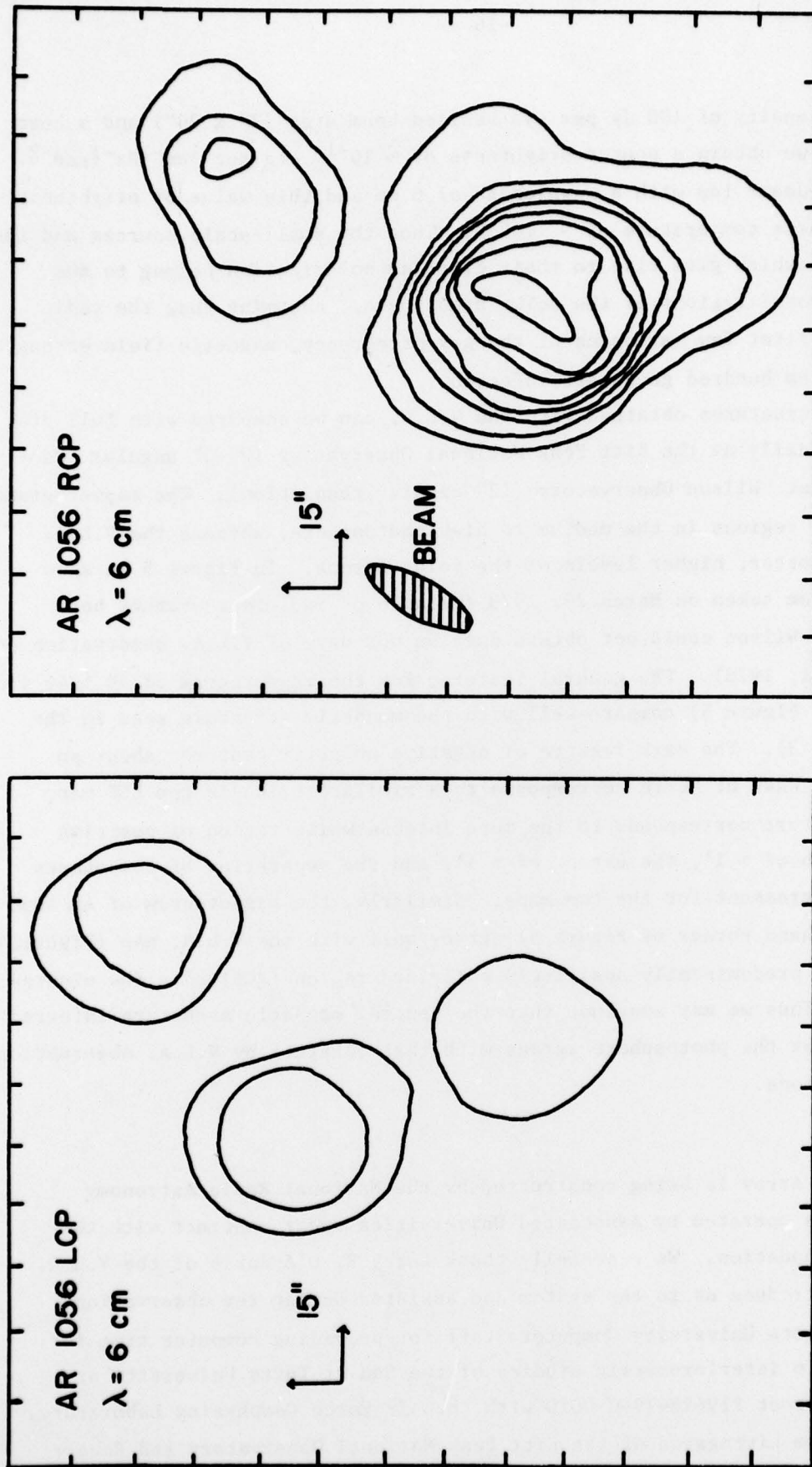


Figure 4. V.L.A. synthesis maps of solar active region 1056 obtained with one day's observation on April 1, 1978. Here, north is up, west is to the right, and LCP and RCP respectively denote the left and right hand circularly polarized signals.

of 30" x 30" an intensity of 100 Jy per synthesized beam area (7" x 20") and a beam efficiency of 80%, we obtain a source brightness of $\sim 10^{-11}$ erg sec⁻¹cm⁻²Hz⁻¹rad⁻². Using the Rayleigh-Jeans law with a wavelength of 6 cm and this value of brightness we obtain a brightness temperature of $\sim 10^6$ K. Thus the small-scale sources and the magnetic structures which give rise to their circular polarization belong to the higher, hotter, coronal regions of the solar atmosphere. Assuming that the radio emission is at the first few harmonics of the gyrofrequency, magnetic field strengths on the order of a few hundred gauss are inferred.²

The magnetic structures obtained with the V.L.A. can be compared with full disk magnetograms taken daily at the Kitt Peak National Observatory (2"-3" angular resolution) and the Mount Wilson Observatory (12" angular resolution). The magnetograms refer to the cooler regions in the medium to high photosphere, whereas the V.L.A. maps refer to the hotter, higher levels of the solar corona. In Figure 5 we show a Kitt Peak magnetogram taken on March 29, 1978 (because of inclement weather both Kitt Peak and Mount Wilson could not obtain data on our days of V.L.A. observation on March 30 and April 1, 1978). The general features for the magnetogram of AR 1046 (in the lower center of Figure 5) compare well with the magnetic structure seen in the V.L.A. maps (Figure 3). The dark feature of negative polarity centered about an axis inclined $\sim 45^\circ$ West of North corresponds to a similar region in the LCP map, whereas the RCP feature corresponds to the more intense white region of positive polarity. The width of $\sim 1'$, the extent of $\sim 4'$, and the separation of components (30" - 1') are in agreement for the two maps. Similarly, the magnetogram of AR 1056 (in the upper left hand corner of Figure 5) agrees well with the V.L.A. map (Figure 4), for both indicate a predominantly positively polarized region (RCP) of a few minutes of arc in extent. Thus we may conclude that the general magnetic structure inferred from magnetograms for the photosphere agrees with that obtained by V.L.A. observations for the coronal regions.

The Very Large Array is being constructed by the National Radio Astronomy Observatory which is operated by Associated Universities under contract with the National Science Foundation. We especially thank Larry R. D'Addario of the V.L.A. staff who helped introduce us to the system and assisted during the observations. We also thank the Tufts University Computer Staff for providing computer time for data analysis. Radio interferometric studies of the Sun at Tufts University are supported under contract F19628-79-C-0010 with the Air Force Geophysics Laboratory. We also thank William Livingston of the Kitt Peak National Observatory and Robert Howard of the Mount Wilson Observatory for supplying us with magnetogram data.

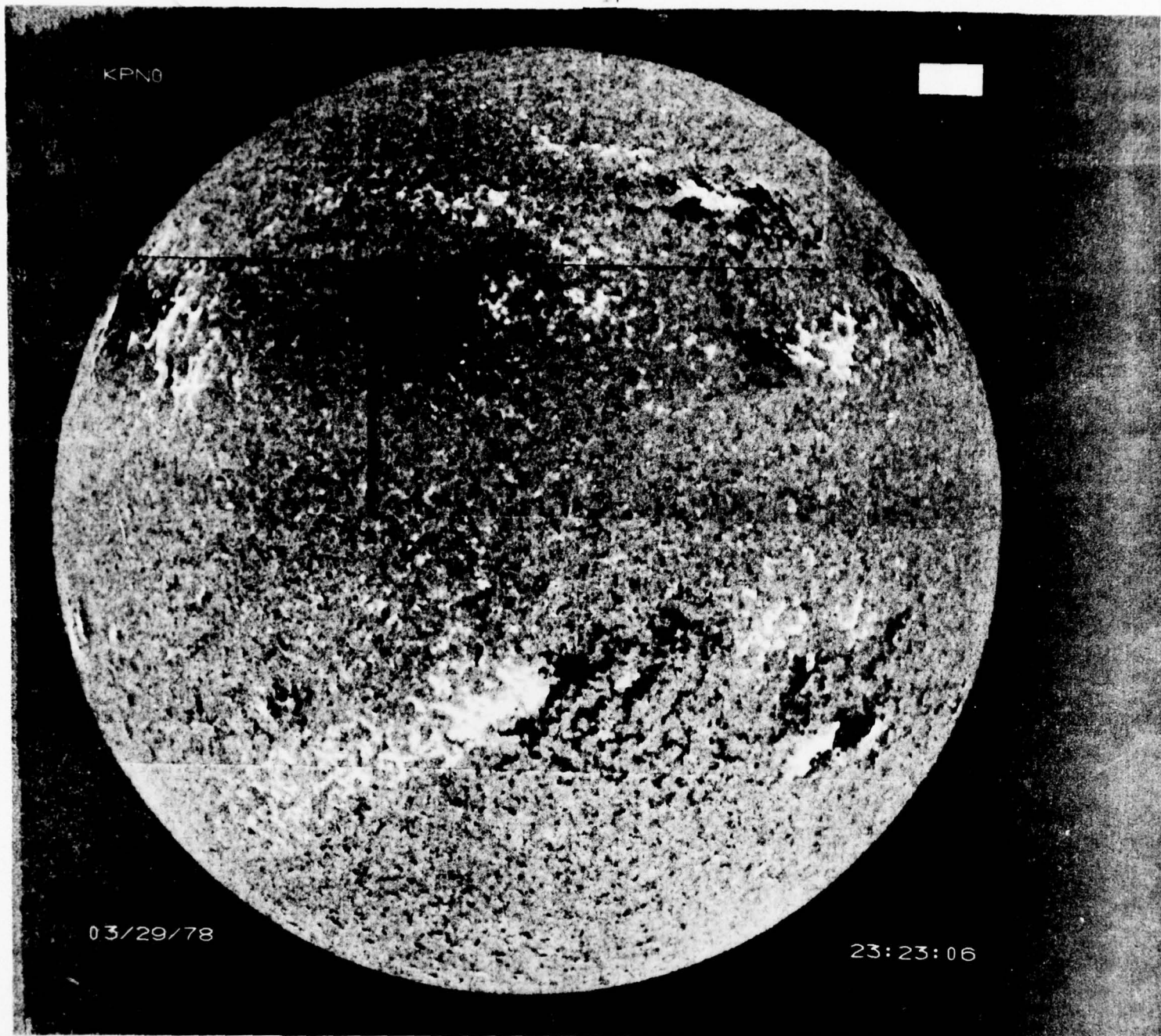


Figure 5. A Kitt Peak National Observatory magnetogram of the sun taken on March 29, 1978. Here, Zeeman effect observations of the 3680 Å line of neutral iron have been used to derive magnetic field structure which is limited by scintillation to 2"-3" angular resolution. As in Figures 3 and 4, north is up and west is to the right, and the dark and light regions respectively refer to regions of negative and positive polarity. The angular scale for the magnetogram is determined by the 32' angular diameter of the sun. The general features of AR 1046 (lower center) and AR 1056 (upper left) compare well with the V.L.A. maps shown in Figures 3 and 4.

REFERENCES

1. Kundu, M.R., Becker, R.H., and Velusamy, T. Solar Phys. 34, 185 (1974).
2. Lang, K.R. Solar Phys. 36, 351 (1974).
3. Stepanov, K.N. Sov. Phys. JETP 8, 195 (1959).
4. Kakinuma, T. and Swarup, G. Astrophys. J. 136, 975 (1962).
5. Zheleznyakov, V.V. Sov. Astron. A.J. 6, 3 (1962), Radio Emission of the Sun and Planets (Pergamon Press, New York, 1970).
6. Lang, K.R. Astrophysical Formulae (Springer-Verlag, Heidelberg, 1974).
7. Fomalont, E.B. and Wright, M.C.H. "Interferometry and Aperture Synthesis" in Galactic and Extra-Galactic Radio Astronomy, ed. G.L. Verschuur and K. I. Kellerman (Springer-Verlag, New York, 1974).
8. Kundu, M.R. and Alissandrakis, C.E. Nature 257, 465 (1975).
9. Kundu, M.R. Alissandrakis, C.E., Bregman, J.D. and Hin, A.C. Astrophys. J. 213, 278 (1977).
10. Heeschen, D.S. Sky and Telescope 49, 344 (1975).
11. Weinreb, S., Ballister, M., Maas, S. and Napier, P.J. IEEE Trans. Micro Thry. Tech MTT-25, 243 (1977).
12. Hogbom, J.A. Astron. and Astrophys. Suppl. 15, 417 (1974).

Printed by
United States Air Force
Hanscom AFB, Mass. 01731